Electronic Supplementary Material (ESI) for Journal of Materials Chemistry A.
This journal is © The Royal Society of Chemistry 2021

Supplementary Information

Bonding Heterogeneity in Mixed-Anion Compounds Realizes Ultralow Lattice Thermal Conductivity

Naoki Sato, Norihide Kuroda, Shun Nakamura, Yukari Katsura, Ikuzo Kanazawa, Kaoru Kimura, and Takao Mori*

Dr. N. Sato
International Center for Young Scientists (ICYS), National Institute for Materials Science (NIMS)
1-2-1 Sengen, Tsukuba, Ibaraki 305-0047, Japan
E-mail: SATO.Naoki@nims.go.jp.

Dr. N. Sato, Prof. Dr. T. Mori
International Center for Materials Nanoarchitectonics (WPI-MANA), NIMS
1-1 Namiki, Tsukuba, Ibaraki 305-0047, Japan

N. Kuroda, S. Nakamura, Prof. Dr. I. Kanazawa
Department of Physics, Tokyo Gakugei University
4-1-1 Nukuikitamachi, Koganei, Tokyo 184-8501, Japan

Dr. Y. Katsura
Research and Services Division of Materials Data and Integrated System (MaDIS), NIMS
1-1 Namiki, Tsukuba, Ibaraki 305-0047, Japan

Prof. Dr. K. Kimura, Dr. Y. Katsura
Department of Advanced Materials Science, The University of Tokyo
5-1-5 Kashiwanoha, Kashiwa, Chiba 277-8561, Japan

Prof. Dr. K. Kimura
OPERANDO-OIL, National Institute of Advanced Industrial Science and Technology (AIST)
5-1-5 Kashiwanoha, Kashiwa, Chiba 277-8561, Japan

Prof. Dr. T. Mori
Graduate School of Pure and Applied Science, University of Tsukuba
1-1-1 Tennodai, Tsukuba, Ibaraki 305-8671, Japan

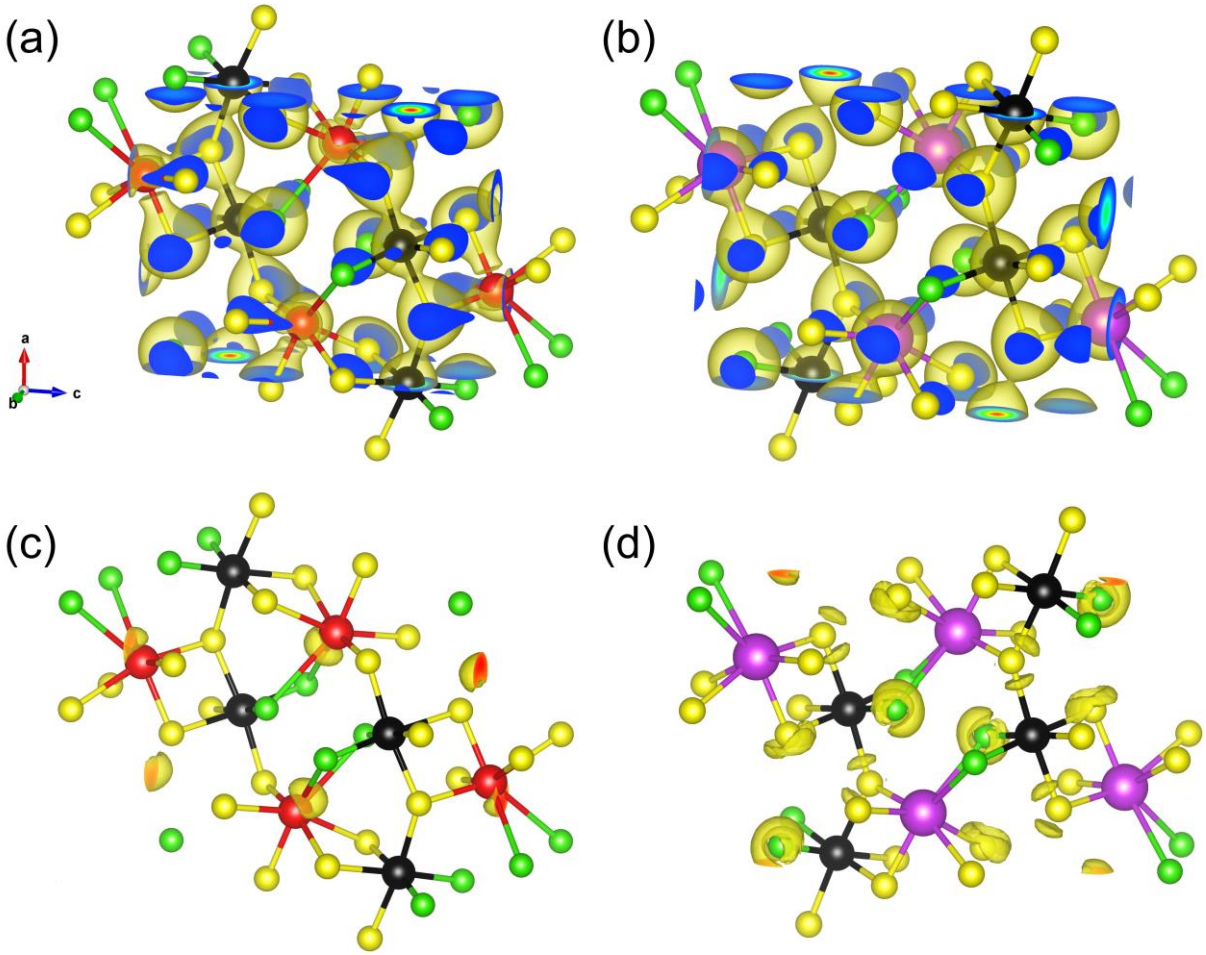

Figure S1. The total charge density of (a) $MnSbS_2Cl$ and (b) $MnBiS_2Cl$ with isosurface value of 0.05 e $bohr^{-3}$, and the electron localization function (ELF) of (c) $MnSbS_2Cl$ and (d) $MnBiS_2Cl$ with isosurface value of 0.80 for (c) and 0.72 for (d), respectively. The black, red, purple, yellow, and green atoms represent Mn, Sb, Bi, S, and Cl, respectively.

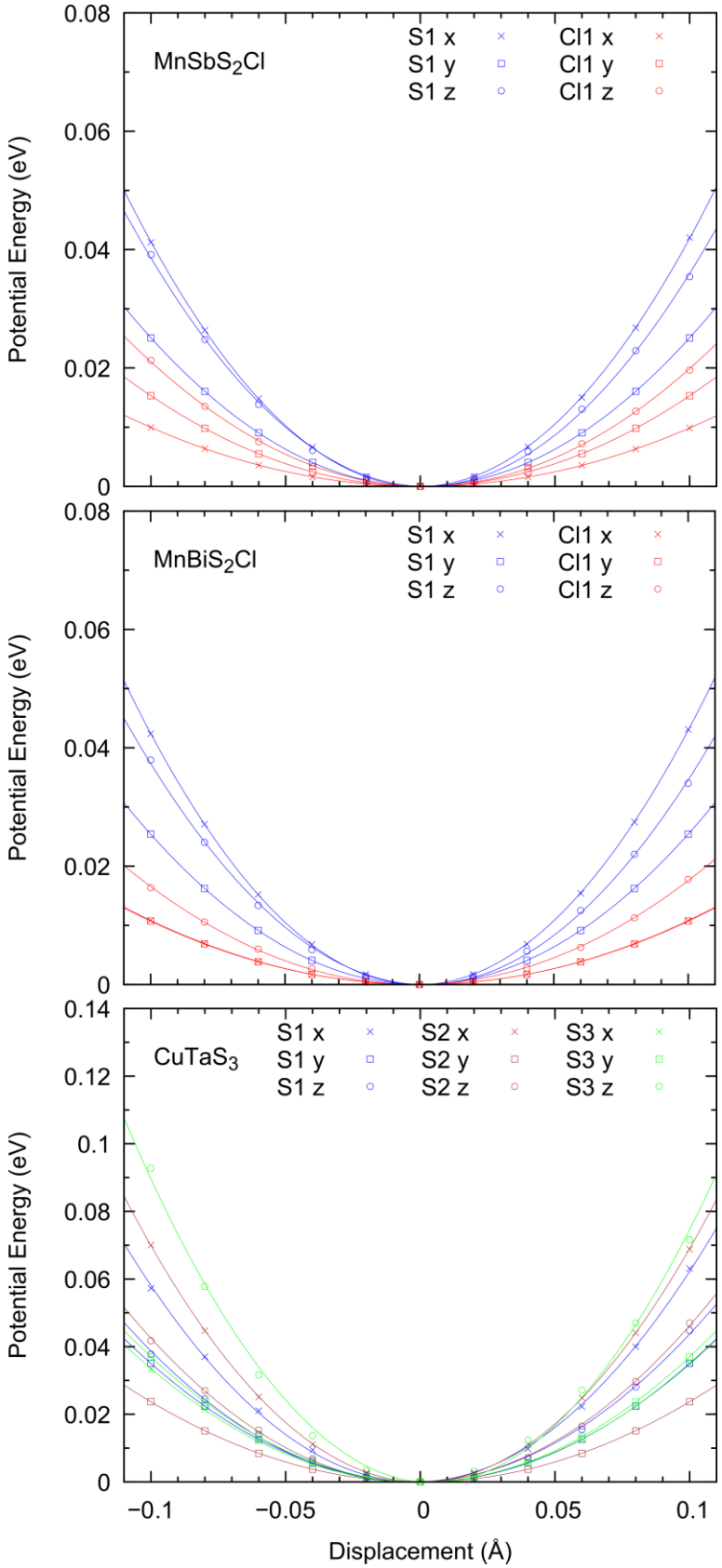

Figure S2. The calculated potential energy of each atomic site as a function of displacements along cartesian *x*-, *y*-, and *z*-directions for $MnSbS_2Cl$, $MnBiS_2Cl$, and $CuTaS_3$ with fitting curves using only quadratic term.

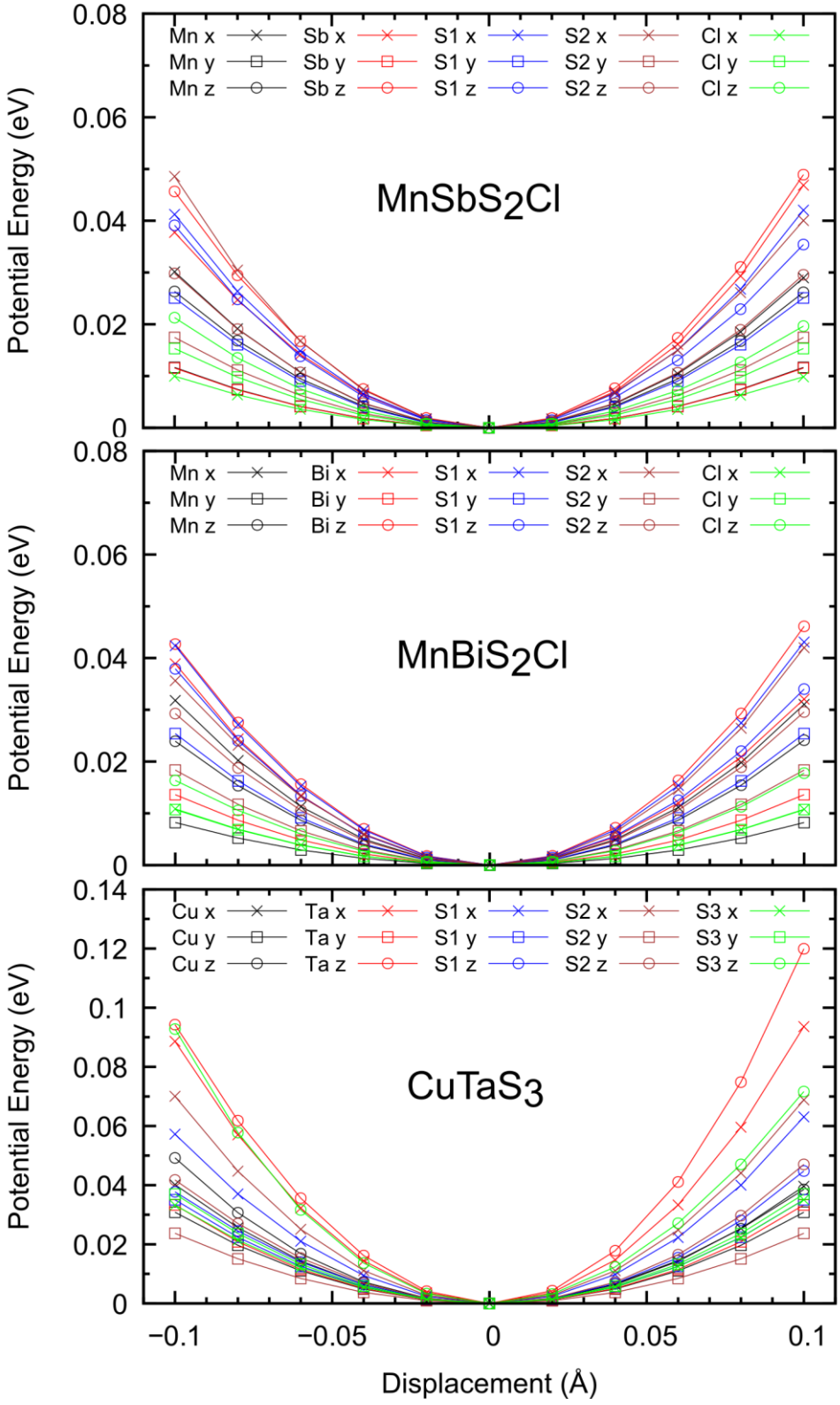

Figure S3. The calculated potential energy of each atomic site as a function of displacements along cartesian *x*-, *y*-, and *z*-directions for $MnSbS_2Cl$, $MnBiS_2Cl$, and $CuTaS_3$.

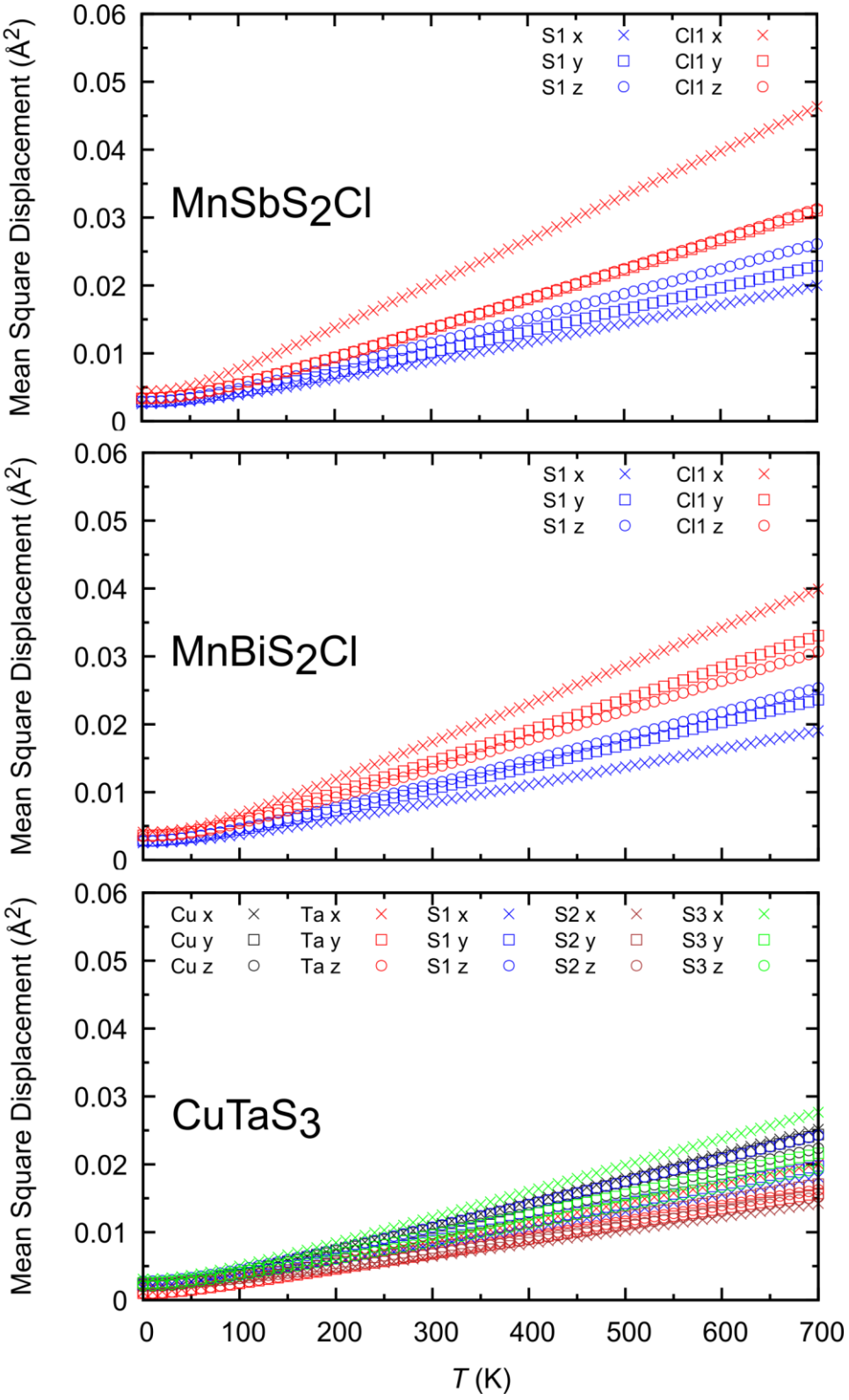

Figure S4. The calculated mean square displacement as a function of temperature along cartesian *x*-, *y*-, and *z*-directions for $MnSbS_2Cl$, $MnBiS_2Cl$, and $CuTaS_3$.

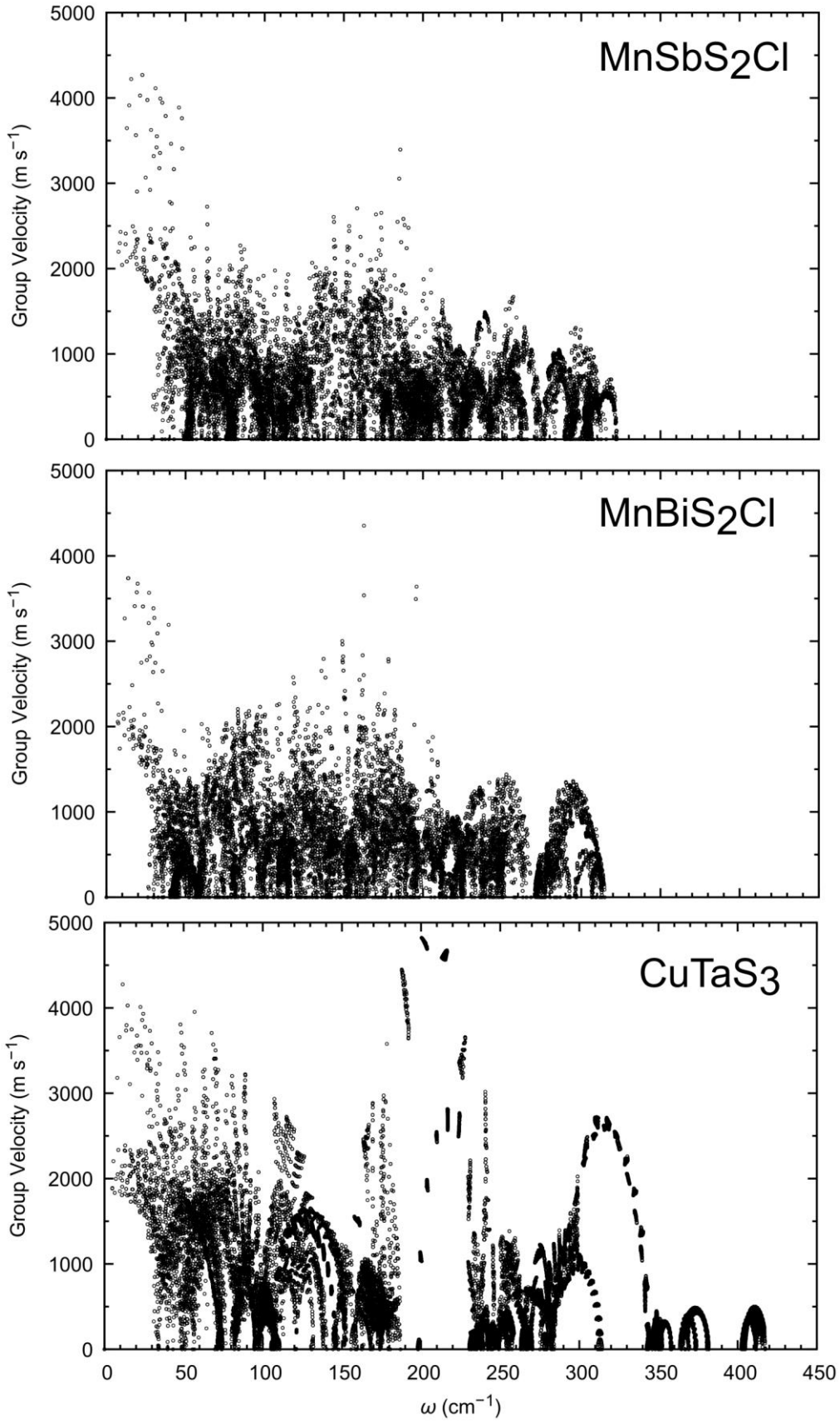

Figure S5. The calculated phonon group velocity as a function of the phonon frequency for $MnSbS_2Cl$, $MnBiS_2Cl$, and $CuTaS_3$.

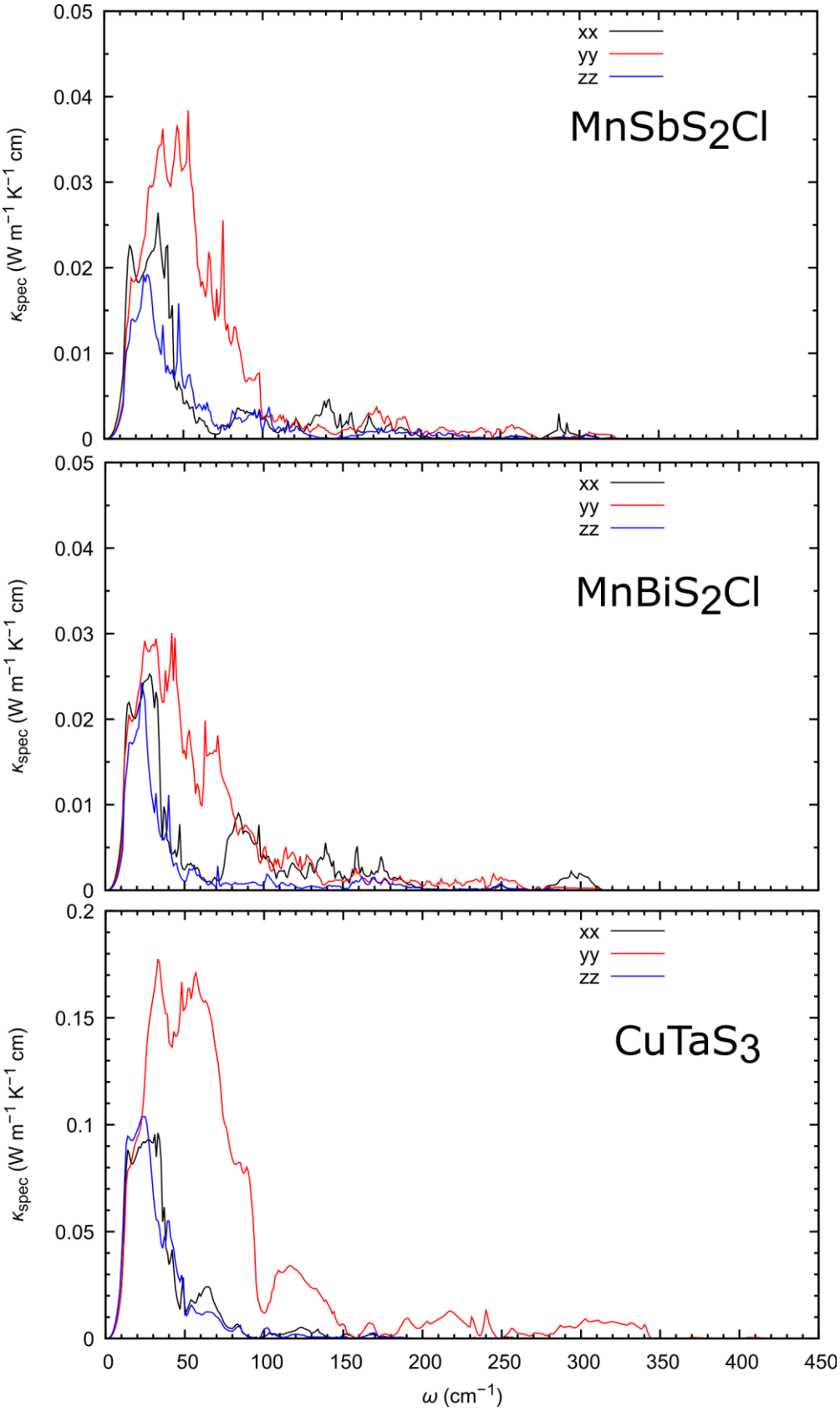

Figure S6. The calculated spectral lattice thermal conductivity, κ_{spec}, as a function of the phonon frequency for $MnSbS_2Cl$, $MnBiS_2Cl$, and $CuTaS_3$.

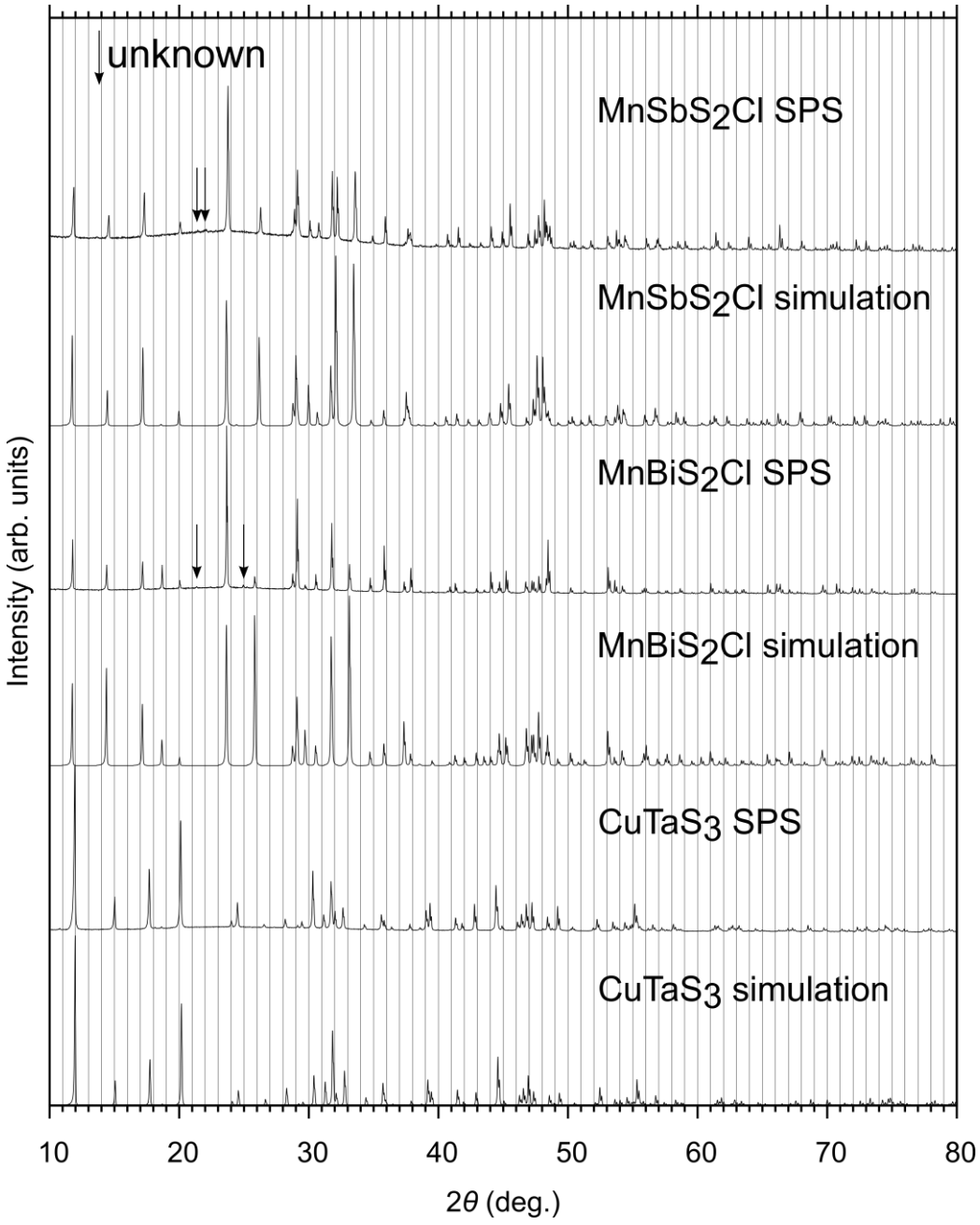

Figure S7. The XRD patterns of the polycrystalline bulk samples prepared by SPS for $MnSbS_2Cl$, $MnBiS_2Cl$, and $CuTaS_3$, together with their simulated patterns. Black arrows denote unknown impurity phases.

Table S1. Lattice parameters of the relaxed primitive cell of $MnSbS_2Cl$, $MnBiS_2Cl$, and $CuTaS_3$.

Material	*a* (Å)	*b* (Å)	*c* (Å)
$MnSbS_2Cl$	9.1800	3.7704	12.039
$MnBiS_2Cl$	9.1672	3.8346	12.111
$CuTaS_3$	9.3918	3.4628	11.688